TIP60 governs the auto-ubiquitination of UHRF1 through USP7 dissociation from the UHRF1/USP7 complex

Tanveer Ahmad
Universite de Strasbourg
Waseem Ashraf
Universite de Strasbourg
Abdulkhaleg Ibrahim
Institut de Genetique et de Biologie Moleculaire et Cellulaire
Liliyana Zaayter
Universite de Strasbourg
Christian D. Muller
Universite de Strasbourg
Ali Hamiche
Institut de Genetique et de Biologie Moleculaire et Cellulaire
Yves Mély
Universite de Strasbourg
Christian Bronner
Institut de Genetique et de Biologie Moleculaire et Cellulaire
Marc Mousli (marc.mousli@unistra.fr)
Universite de Strasbourg

Research

Keywords: Cancer, Epigenetics, UHRF1, TIP60, USP7, Ubiquitination, Fluorescence lifetime imaging microscopy (FLIM), Protein-protein interaction, Apoptosis

Posted Date: September 1st, 2020

DOI: https://doi.org/10.21203/rs.3.rs-66228/v1

Abstract

Background: The epigenetic regulator UHRF1 (Ubiquitin-like, containing PHD and RING finger domains 1) plays an essential role in faithful transmission of DNA methylation during replication. It has tumorogenesis potential and is overexpressed in cancers. TIP60 (Tat interactive protein, 60 kDa) is an important partner of UHRF1, ensuring various cellular processes through its acetyltransferase activity. TIP60 is believed to exert a tumor suppressive role partly explained by its down-regulation in many cancers. Both proteins participate in various cellular functions such as chromatin remodeling, cell cycle, DNA damage repair and regulation of protein stability.

Methods: Immunoprecipitation and confocal microscopy techniques were performed to study the ubiquitination of UHRF1 and USP-UHRF1 association. Fluorescence lifetime imaging microscopy (FLIM) technique was performed to analyze the interaction between UHRF1 and ubiquitin inside the nucleus. Western blotting was used to assess the effect of TIP60 overexpression on p73, pro- and anti-apoptotic proteins. TIP60-mediated apoptosis in HeLa cells was investigated by flow cytometry. Results were statistically analyzed using Graphpad prism.

Results: Herein, our goal was to investigate the role and mechanism of TIP60 in the regulation of UHRF1 expression. Our results showed that TIP60 overexpression down-regulated UHRF1 and DNMT1 (DNA methyltransferase 1) expressions. TIP60 interfered with USP7-UHRF1 association and induced degradation of UHRF1 in an auto-ubiquitination dependent pathway. Moreover, TIP60 activated the p73-mediated apoptotic pathway.

Conclusion: Taken together, our data suggest that the tumor suppressor role of TIP60 is mediated by its regulation to UHRF1.

Background

The multidomain protein, Ubiquitin-like, containing PHD and RING finger domains 1 (UHRF1, also known as ICBP90 in human) [1, 2], is an important epigenetic integrator responsible for the faithful transmission of DNA methylation patterns from parent strands to daughter strands during DNA replication [1, 3, 4, 5, 6, 7, 8]. UHRF1 performs this role by recognizing the CpG motifs in hemi-methylated DNA through its SRA domain (SET and RING-associated domain) and by recruiting DNMT1 (DNA methyltransferase 1) [6, 7, 8, 9, 10]. TTD and PHD domains help UHRF1 to read the histone marks [11, 12, 13]. The RING domain of UHRF1 has intrinsic ubiquitin E3 ligase activity by which UHRF1 can ubiquitinate itself (auto-ubiquitination) [14, 15] or other proteins including histones [16, 17]. Ubiquitylation by UHRF1 of H3K23 and H3K18 is important to create binding sites for DNMT1 [7, 18, 19, 20, 21]. The N-terminal UBL domain of UHRF1 binds directly to DNMT1 and increases its enzymatic activity toward chromatin by controlling H3 ubiquitination [20, 21, 22]. UHRF1 is also involved in DNA damage response [4, 23, 24] and regulation of the stability and function of several other proteins such as p53, PML (promyelocytic leukemia protein) and DNMT1 through the collaboration with other epigenetic partners such as USP7 (Ubiquitin-specific-

processing protease 7), HDAC1 (histone deacetylase 1) and TIP60 (Tat interactive protein, 60 kDa) [4, 17, 25, 26].

We first reported the interaction of UHRF1 with TIP60 [27]. Indeed, UHRF1 and TIP60 were found to be in the same macromolecular complex and interact with each other [17, 25, 27]. TIP60 was originally recognized as an interacting partner of HIV-1 Tat protein [28]. TIP60 (also known as KAT5) belongs to the MYST family (MOZ, YBF2/SAS3, SAS2, TIP60) having an evolutionary conserved domain which harbors histone acetyltransferase (HAT) activity [29, 30, 31, 32]. At its N-terminus, TIP60 has a chromodomain (CRD), while its C-terminus contains the conserved enzymatic MYST domain [33]. TIP60 reads histone marks (H3K4me2/H3K9me3) through its CRD domain [34] and translates it through MYST domain [35]. Inside the MYST domain, there is the catalytic HAT domain which binds to acetyl coenzyme A and catalyzes acetylation of both histone and non-histone proteins [36, 37]. This acetyltransferase activity is stimulated by a zinc finger which helps TIP60 to interact with the targeted substrates [38, 39, 40]. Through its enzymatic activity, TIP60 is a central player in many key cellular processes like chromatin remodeling, DNA damage response, transcription regulation, genomic integrity, cell cycle and apoptosis [25, 36, 39, 41, 42, 43]. For instance, it interacts with and regulates transcription of nuclear hormone receptors, p53, c-MYC and NF-κB [39, 42, 44]. Interestingly, it also regulates p53 activity in an acetylation-dependent (K120 of p53) and independent way [25]. Acetylation of p53 activates p21 and the PUMA pathway, which leads to cell growth arrest and apoptosis, and thus, ensures tumor suppression [25].

Downregulation of TIP60 inhibits both p21 activation and growth arrest [45]. During M-phase, TIP60 is essential for the chromosomal segregation [46] and cell cycle progression [47, 48, 49]. Cells lacking TIP60's acetyltransferase activity, loose their ability to repair DNA and ultimately, the cell cycle control [41]. Heterozygous deletion of TIP60 gene (*HTATIP*) has a lethal effect on embryos [50]. In many cancers, TIP60 levels are low as compared to normal cells supporting a tumor suppression role [25, 41, 45, 51, 52, 53, 54, 55, 56]. In accordance with this role, high levels of UHRF1 have been shown to interfere with TIP60-p53 interplay and prevent p53 activation which leads to tumorogenesis and/or tumor progression [25]. Therefore, targeting UHRF1 in cancer cells would permit to rescue p53 levels and enhance the coordinated dialogue between p53 and TIP60. In a previous study, we have shown that UHRF1 interacts with the MYST domain of TIP60 [57]. Moreover, UHRF1 through its E3 ligase activity, ubiquitinates DNMT1 and by this way impacts its levels [17, 58, 59]. Although it has already been shown that TIP60 overexpression down regulates UHRF1 levels in HeLa cells [57], the mechanism of the TIP60-mediated UHRF1 down-regulation in cancer cells remains elusive. Here, we demonstrate that TIP60 interferes with the UHRF1-USP7 association. After dissociation from USP7, UHRF1 is auto-ubiquitinated by its RING domain. The resulting down-regulation of UHRF1 activates p73- mediated apoptosis. Altogether, these observations provide new insights about TIP60's tumor suppressive role by controlling UHRF1 levels.

Methods

Materials

MG-132 ($C_{26}H_{41}N_3O_5$) was purchased from Selleckchem.com Inhibitor Expert (S2619, USA). MG-132 was dissolved in pure DMSO (Sigma-Aldrich) and stored at -80 °C. Propidium iodide (130-093-233) was purchased from Miltenyi Biotec while Annexin V-iFluor™ 350 conjugate (20090) was purchased from AAT Bioquest^R. TIP60 inhibitor 5-(1,2-Thiazol-5-yldisulfanyl)-1,2-thiazole (NU9056) was purchased from TOCRIS (1450644-28-6).

Cell culture

HeLa cells (ATCC, CCL-2, Amp, Cervical Adenocarcinoma; Human) and HeLa cells stably expressing either GFP-UHRF1 WT or GFP-UHRF1 C724A-H741A protein, were grown in Dulbecco's Modified Eagle's Medium (DMEM 1X + GlutaMAX™, Pyruvate, Gibco, Lifetech, France) which was supplemented with 10% fetal bovine serum (FBS, S1810-500, Dominique Dutscher), in addition to mixture of penicillin (100 U/ml) and streptomycin (100 U/ml) (17-602E, Lonza, USA), at 37 °C with 5% CO_2 in humidified environment. Plasmids were transfected in HeLa cells with either jetPEI™ or jetPRIME (PolyPlus-transfection, France) according to the manufacturer's protocol.

Plasmid constructs

TIP60 wild-type and mutants (ΔHAT, ΔMYST) were cloned into a pEGFP-N1 plasmid to express eGFP-labeled TIP60 proteins in HeLa cells. RFP-Ubiquitin was purchased from addgene (#11935).

Antibodies

Mouse monoclonal anti-UHRF1 was engineered as described previously [1]. Other antibodies used include rabbit polyclonal anti-HAUSP/USP7 (Abcam, ab4080), mouse monoclonal anti-DNMT1 (Proteogenix, France, PTG-MAB0079), mouse monoclonal anti-Ubiquitin (Merck, 05-944), mouse monoclonal eGFP (Proteintech, 66,002-1-Ig and Thermo Fisher Scientific A-11120), rabbit polyclonal anti-mCherry (Genetex GTX 59788), mouse monoclonal anti-GAPDH (Merck Millipore MAB374), mouse monoclonal anti-GFP (Proteintech, 66002-1-Ig), mouse monoclonal anti-p73 (BD Biosciences Pharmingen, 558785), rabbit polyclonal anti-Caspase 3 (Cell Signaling Technology, Danvers, MA, USA, 9661), mouse monoclonal anti-BCL2 (Merck-Millipore, 05-826), mouse monoclonal anti-PARP (BD Biosciences Pharmingen, 51-6639GR) and rabbit polyclonal anti-BAX (Merck Millipore, AB2930).

Western blotting

For Western blot, cells were collected 24 h after the transfection by trypsinization. For ubiquitination experiments, cells were treated with MG-132 (10 μM) 8 h before cells harvesting. After centrifugation, media was discarded, and cell pellet was washed with PBS. Cells were lysed with ice cold lysis buffer (10 mM Tris-HCl pH 7.5, 1 mM EDTA, 150 mM NaCl and 1% NP40 supplemented with protease inhibitors (11836170001, cOmplete mini EDTA-free protease inhibitor cocktail tablets, Roche Diagnostics GmbH, Germany). After denaturation for 7 min in Laemmli sample buffer (1610747, Bio-Rad Laboratories USA), 40 μg of the protein from cell lysates were loaded on 7.5% and 10% SDS-PAGE gels. Proteins were identified by anti-UHRF1, anti-Ubiquitin, anti-DNMT1, anti-USP7, anti-eGFP and anti-GAPDH antibodies, with overnight incubation at 4 °C. HRP (horseradish peroxidase) conjugated secondary antibodies, anti-

mouse (W402B, Promega, France) or anti-rabbit (W401B, Promega, France) were used to label primary antibodies. Signals were detected on an Image Quant LAS 4000 apparatus (GE Healthcare Life Sciences, USA) with chemiluminescent ECL system (Clarity™ ECL western blotting substrate, Bio-Rad, France, 170–5060). Image Studio Lite (Li-Core Biosciences, USA) was used to analyze the images.

Immunoprecipitation (IP)

For immunoprecipitation, cells were collected and lysed by freeze shock. Mild sonication was done in ice cold PBS freshly supplemented with protease inhibitors cocktail tablet. Input controls were made by taking 40 µg of protein from each lysate. 1000 µg to 1500 µg of protein lysate were incubated with anti-UHRF1 antibody at 4 °C for 3 h or with anti-USP7 antibody at 4 °C overnight. After washing and equilibration, 60 µL of Dynabeads® protein A (Thermo Fischer Scientific, Norway 1002D) were added to the lysate-antibody mixture and incubated for 1 h at 4 °C. Later, beads were collected and washed 3–5 times with ice cold PBS freshly supplemented with protease inhibitors tablet. Finally, beads were resuspended in Laemmli sample buffer. Proteins were denatured by heating at 95 °C for 7 min and analyzed through Western blotting.

UHRF1 auto-ubiquitination assay

HeLa cell lines stably expressing GFP-UHRF1 wild-type and GFP-UHRF1 C724A-H741A mutant proteins, were prepared as described elsewhere [15]. HeLa cells stably expressing GFP-UHRF1 WT and GFP-UHRF1 C724A-H741A mutant proteins were transfected with either TIP60 WT or TIP60ΔMYST mutant using jetPRIME reagent. Samples were treated with 10 µM MG-132, 8 h before harvesting the cells. Immunoprecipitation (as described above) was performed with anti-GFP antibody to immunoprecipitate the GFP-tagged UHRF1 protein. Samples were resolved by Western blotting.

Confocal microscopy

To study the effect of TIP60 overexpression on UHRF1 and DNMT1 levels, HeLa cells were seeded on a cover glass and transfected with eGFP or TIP60-eGFP or TIP60ΔMYST-eGFP plasmids by using jetPEI™ reagent as described in manufacturer's protocol. 24 h post-transfection, cells were fixed with 4% paraformaldehyde for 10 minutes and then, permeabilized with 0.2% Triton X-100 for 20 min at room temperature. Next, blocking was done with 1% BSA for 1 hour, before incubation with a primary antibody against either UHRF1 or DNMT1 for 3 h at 4 °C. After washing three times with PBS, cells were incubated with secondary antibody labeled with Alexa Fluor 568 (goat anti-mouse, A11031, Invitrogen) for 60 min at room temperature. Next, cells were washed three times and labeled with DAPI (Hoechst stain 33258, Molecular probes). Finally, cells were imaged with a confocal Leica TCS SPE microscope equipped with a 20 × air (0.7 NA) immersion lens objective. For DAPI, Alexa Fluor 568 and eGFP, excitation was performed with a 405 nm laser (25 mW), 561 nm laser (10 mW) and 488 nm laser (25 mW), respectively. The detection range for the three dyes was 430–480 nm, 570–630 nm and 500–523 nm, respectively.

To check the effect of TIP60 overexpression on the co-localization of UHRF1 and Ubiquitin, HeLa cells were co-transfected with either eGFP and RFP-Ubiquitin or TIP60-eGFP and RFP-Ubiquitin by using

jetPEI™ reagent. One group of samples was treated with MG-132 (10 μM) 8 h before cell fixation, to block the proteasomal degradation of UHRF1. Cells were labeled with anti-UHRF1 as primary antibody and Alexa Fluor 647-labelled goat anti-mouse, A21237 (Molecular probes) as secondary antibody. DAPI staining was done to visualize the nucleus. All samples were imaged with a confocal Leica TCS SPE equipped with an oil immersion objective (HXC PL APO 63×/1.40 OIL CS). For DAPI, RFP, Alexa Fluor 647 and eGFP, excitation was performed with a 405 nm laser (25 mW), 561 nm laser (10 mW), 635 nm laser (18 mW) and 405 nm laser (25 mW), respectively. The detection range for the four dyes was 430–480 nm, 570–630 nm, 640–702 nm and 500–523 nm, respectively.

For UHRF1-USP7 association study, HeLa cells were transfected with either TIP60-eGFP or TIP60ΔMYST-eGFP by using jetPEI™ reagent. One group of samples was treated with MG-132 (10 μM) 8 h before cell fixation, to block the proteasomal degradation of UHRF1 and USP7. Cells were labeled with anti-UHRF1 (mouse) and anti-USP7 (rabbit) antibodies overnight at 4 °C. Then cells were incubated with secondary antibody labeled with Alexa Fluor 568 (goat anti-rabbit, A11011, Invitrogen) for USP7 and Alexa Fluor 647 (goat anti-mouse) for UHRF1. DAPI staining was done to stain the nucleus. All samples were imaged with a confocal Leica TCS SPE equipped with an oil immersion objective (HXC PL APO 63×/1.40 OIL CS). For DAPI, Alexa Fluor 568, Alexa Fluor 647 and eGFP, excitation was performed with a 405 nm laser (25 mW), 561 nm laser (10 mW), 635 nm laser (18 mW) and 405 nm laser (25 mW), respectively. The detection range for the four dyes was 430–480 nm, 570–625 nm, 644–707 nm and 500–531 nm, respectively. All the images were processed with Image J software.

Fluorescence Lifetime Imaging Microscopy (FLIM)

HeLa cells stably expressing GFP-UHRF1 WT or GFP-UHRF1 C724A-H741A protein, were seeded (10^5 cells per dish) in a μ-dish (Ibidi) with 35 mm wells. Cells were transfected with 1 μg RFP-Ubiquitin plasmid by using jetPEI™ reagent. Cells were fixed with 4% paraformaldehyde. After fixation, cells were imaged with a homemade two-photon excitation scanning microscope based on an Olympus IX70 inverted microscope with an 60 × 1.2 NA water immersion objective operating in the descanned fluorescence collection mode as described [60, 61]. Two-photon excitation at 930 nm was provided by an Insight DeepSee laser (Spectra Physics). Fluorescence photons were collected using a short-pass filter with a cut-off wavelength of 680 nm (F75-680, AHF, Germany) and a band-pass filter of 520 ± 17 nm (F37-520, AHF, Germany). The fluorescence was directed to a fiber coupled APD (SPCM-AQR-14-FC, Perkin Elmer), which was connected to a time-correlated single photon counting module (SPC830, Becker & Hickl, Germany). FLIM data were analyzed using SPCImage v 7.3 (Becker & Hickel) and the Förster resonance energy transfer (FRET) efficiency was calculated according to $E = 1- (\tau_{DA}/\tau_D)$, where τ_{DA} is the lifetime of the donor (GFP) in the presence of acceptor (RFP) and τ_D is the lifetime of GFP in the absence of acceptor.

Apoptosis analysis

Flow cytometry was used to analyze the TIP60-induced apoptosis. HeLa cells were seeded in six well plates. Cells were transfected with TIP60-eGFP by using jetPEI™ reagent. TIP60 transfected cells were compared to control cells or cells treated with jetPEI™ only. Cells were collected after mild trypsinization

and incubated with Propidium iodide (PI) and Annexin V-iFluor^{TM}350 conjugate. Then samples were analyzed with a Guava easyCyte™ flow cytometer (Merck Millipore). The InCyte Software for Guava (Merck Millipore) was used to analyze the results.

Results

TIP60 overexpression induces ubiquitination of UHRF1

We have previously shown that TIP60 overexpression downregulates UHRF1 and DNMT1 [57]. Here, we confirm by confocal microscopy experiments that a significant decrease in UHRF1 and DNMT1 fluorescence intensity was detected in TIP60-eGFP WT transfected cells while TIP60ΔMYST-eGFP transfection only marginally affected UHRF1 and DNMT1 fluorescence intensity (Figure S1).

In Fig. 1, HeLa cells were co-transfected with TIP60-eGFP + RFP-ubiquitin. Non-treated HeLa cells and eGFP + RFP-ubiquitin co-transfected cells served as controls. Endogenous UHRF1 levels were detected by using a specific primary antibody against UHRF1 and Alexa 647-labeled secondary antibody. TIP60, UHRF1 and ubiquitin were well co-localized in the nucleus (Fig. 1). A clearly visible decrease in UHRF1 expression was observed in TIP60 + ubiquitin co-transfected cells as compared to adjacent non-transfected cells in the same sample or control samples (Fig. 1A). Quantification of the mean fluorescence intensity of Alexa 647 revealed a significant decrease in UHRF1 fluorescence intensity (57%) in TIP60 + ubiquitin co-transfected cells (Fig. 1B). The decrease in fluorescence intensity was comparable in both control or eGFP + ubiquitin transfected cells (6%) (Fig. 1B). UHRF1 expression was restored in TIP60 + ubiquitin co-transfected cells treated with the proteasomal inhibitor MG-132 (Fig. 1C). Mean fluorescence intensity of UHRF1 was recovered significantly (Fig. 1D).

Next, we checked the effect of TIP60 overexpression on UHRF1 ubiquitination as a function of time (Fig. 2). HeLa cells were transfected with either TIP60 WT or TIP60ΔMYST mutant. Cells were collected at different time intervals after transfection. Immunoprecipitation was performed with anti-UHRF1 antibody. We observed a prominent ubiquitination smear with ubiquitinated UHRF1 bands after 3 and 6 h post TIP60 WT transfection (Fig. 2B, IP lanes 2 and 3). In contrast, no effect was observed after 12 and 24 h post TIP60 WT transfection suggesting that UHRF1 ubiquitination is transient. In case of TIP60ΔMYST, no ubiquitination of UHRF1 was observed up to 24 h post transfection. These results show that TIP60 overexpression induces a transient ubiquitination that did not lead to degradation of UHRF1, due to proteasome inhibition by MG-132.

TIP60 overexpression induced auto-ubiquitination of UHRF1

The RING Finger domain of UHRF1 has E3 ligase activity through which it can either ubiquitinate itself (autoubiquitination) [14, 15] or other proteins [16, 17]. Therefore, we have investigated whether down-regulation of UHRF1 levels is the consequence of UHRF1 auto-ubiquitination activity or whether other E3 ligases are responsible for this. This experiment was performed using HeLa cells stably expressing either

UHRF1 WT protein or UHRF1 C724A-H741A mutant protein having impaired RING Finger domain activity. Cells were transfected with either TIP60 WT or TIP60ΔMYST mutant and treated with MG-132. We observed poly-ubiquitination of UHRF1 WT when TIP60 WT was over-expressed as compared to either controls or ΔMYST mutant samples (Fig. 3, IP lane 2). Interestingly, in the case of UHRF1 C724A-H741A, no significant ubiquitination smear and bands above UHRF1 band were observed (Fig. 3, IP lane 4,5,6). This indicates that after TIP60 overexpression, UHRF1 is auto-ubiquitinated via its RING Finger. In contrast, UHRF1 bearing the RING Finger domain mutation failed to be auto-ubiquitinated after TIP60 overexpression.

UHRF1 interacts with ubiquitin

We further confirmed the interaction between UHRF1 and ubiquitin inside the cell using FRET (Förster Resonance Energy Transfer) experiments. FRET between GFP- and RFP- labeled proteins only occurs when they are less than 8 nm apart, a distance relative to intermolecular protein-protein interactions [60]. FRET efficiency is deduced from the decrease in GFP fluorescence lifetime measured by Fluorescence Lifetime Imaging Microscopy (FLIM) [61]. FLIM technique allows to derive and color code the fluorescence lifetime (τ) of GFP at each pixel of the image (Fig. 4). In comparison to fluorescence intensity, τ does not depend on the fluorophore concentration or instrumentation. HeLa cells expressing either GFP-UHRF1 WT or GFP-UHRF1 C724A-H741A mutant were used for the experiments.

These cells were co-transfected with RFP-labeled ubiquitin and fixed at different times, between 6 and 24 h. The fluorescence lifetime of GFP-UHRF1 WT used as a control was 2.45 ± 0.01 ns (n = 36 cells) (Fig. 4A a). The lifetime of GFP-UHRF1 was observed to decrease as a function of time when GFP-UHRF1 WT cells were transfected with RFP-ubiquitin (Fig. 4B). A significant decrease in lifetime was observed after 12 h of RFP-ubiquitin transfection (2.25 ± 0.02 ns, n = 26 cells) and a further decrease in lifetime was observed after 24 h (2.00 ± 0.01 ns, 20 cells) (Fig. 4A b). Corresponding FRET efficiency was 8.2 ± 0.8% and 19.4 ± 0.3% after 12 and 24 h of RFP-ubiquitin transfection, respectively. Next, we checked the interaction between RFP-labeled ubiquitin and GFP-labeled UHRF1 having a RING Finger domain mutation, as a function of time. The lifetime of GFP-UHRF1 C724A-H741A taken as control was 2.47 ± 0.01 ns (28 cells) (Fig. 4A c). Interestingly, we did not observe any significant decrease in the lifetime of GFP-UHRF1 C724A-H741A after RFP-ubiquitin transfection. After 24 h of RFP-ubiquitin transfection, the lifetime was 2.42 ± 0.01 ns (18 cells) (Fig. 4A d), which corresponded to a FRET efficiency of 2.0 ± 0.3%, below the commonly accepted 5% threshold value for protein-protein interaction [62]. Thus, our data suggest that mutation in the RING Finger domain of UHRF1 can impair its interaction with the ubiquitin.

Further, we decided to study the effect of inhibition of TIP60's acetylation activity on the interaction between UHRF1 and ubiquitin, by using the specific TIP60 inhibitor, NU9056. First, we studied the effect of NU9056 at different concentrations between 1 and 100 μM after 24 h treatment and we analyzed UHRF1-ubiquitin interaction through FLIM, using HeLa cells expressing GFP-UHRF1 WT protein. The interaction between UHRF1 and ubiquitin could be still detected in the presence of 1, 3, and 5 μM of NU9056 (FRET efficiency was 12, 10, and 8.8%, respectively), but was impaired significantly at 10, 30 and

100 μM (FRET efficiency 5.6, 4.8 and 3.6% respectively) (Figure S2). Further experiments were carried out to investigate the effect of NU9056 on UHRF1-Ubiquitin interaction in a time dependent manner at 10 μM and 100 μM. Under these conditions, we did not observe a significant decrease in lifetime of GFP-UHRF1 at any time-intervals in the presence of TIP60 inhibitor as shown in Fig. 4A (e and f). Overall, our FLIM data suggest that TIP60 favors UHRF1-Ubiquitin interaction while inhibition of acetyltransferase activity of TIP60 results in impairment of this interaction.

TIP60 overexpression interferes with USP7-UHRF1 association

In order to decipher the origin of the activation of UHRF1 auto-ubiquitination, we hypothesized an alteration of the protective role of USP7. Indeed, USP7 interacts with UHRF1 and protects it from ubiquitin-mediated proteasomal degradation [58, 64]. To assess this hypothesis, HeLa cells were transfected with either TIP60-eGFP or TIP60ΔMYST-eGFP mutant. Anti-UHRF1 antibody was used to immunoprecipitate the endogenous UHRF1 and its associated partner USP7. Association between USP7 and UHRF1 was observed in the untreated sample (control) as USP7 was co-immunoprecipitated with UHRF1 (Fig. 5D). In TIP60 overexpressed sample, USP7 was barely detected after co-precipitation with UHRF1 (Fig. 5D, lane 2). In contrast, with TIP60ΔMYST-eGFP mutant this association was not affected (Fig. 5D, lane 3). In a reciprocal experiment, anti-USP7 antibody was used to immunoprecipitate the endogenous USP7. We observed that after TIP60 WT overexpression, reduced levels of endogenous UHRF1 were co-precipitated as compared to control and TIP60ΔMYST-eGFP mutant sample (Fig. 5E, compare lane 2 to lanes 1 and 3). Together, these results suggest that TIP60 regulates the interaction of UHRF1 with USP7, which conditions the auto-ubiquitination activity of UHRF1.

Quantitative analysis of the input fractions (Fig. 5A)revealed a significant decrease in UHRF1, USP7 and DNMT1 levels after TIP60 WT overexpression (Fig. 5B). MG-132 treatment fully restored USP7 and DNMT1 but only partially UHRF1 levels (Fig. 5C). To check the expression levels of USP7 and UHRF1 inside the cells after TIP60 overexpression, we performed confocal microscopy experiments. The endogenous levels of UHRF1 and USP7 were checked in the same cells by labeling with respective antibodies. Based on the mean fluorescence intensity of Alexa 568- and Alexa 647-labeled secondary antibodies, USP7 and UHRF1 levels were found to decrease significantly after TIP60 overexpression (Fig. 6A, C). As compared to the control samples, fluorescence drops of 45% and 60% were observed for USP7 and UHRF1, respectively. In contrast, overexpression of the TIP60ΔMYST-eGFP mutant only marginally affected the fluorescence intensities of USP7 and UHRF1 (Fig. 6A, C). Thus, our data demonstrate that TIP60 overexpression can down-regulate USP7 and UHRF1 levels simultaneously. Due to its down-regulation, USP7 was likely unable to protect the UHRF1 degradation via proteasomal pathway. As we observed a significant decrease in USP7 levels after TIP60 overexpression, we further checked USP7 levels after treatment with MG-132. Interestingly, expression levels of USP7 were significantly improved in TIP60 overexpressed samples after treatment with MG-132 (Fig. 6B, D). Expression levels of UHRF1 were also improved but to a lesser extent as compared to USP7, which

suggests that once UHRF1 is degraded through the proteasomal degradation pathway, its levels are not restored immediately (Fig. 6B, D).

TIP60 overexpression induces activation of p73

Since our experiments indicate that TIP60 regulates UHRF1 expression by governing its auto-ubiquitination, we next investigate the physiological or physiopathological consequences of this regulation. Tumor suppressor protein p73 is important for genomic stability by responding to a number of stress signals and is under the control of UHRF1 [65, 66]. The p73-mediated apoptosis leads to activation of mitochondria dependent apoptotic pathway through transactivation of pro-apoptotic proteins (e.g. BAX) and downregulation of pro-survival proteins (*e.g.* BCL2) [67, 68]. Therefore, we investigated the effect of UHRF1 downregulation. We found that overexpression of TIP60 induces a significant increase in the expression of p73 (Fig. 7A) and BAX protein (Fig. 7B), but a decrease in the expression of anti-apoptotic BCL2 protein (Fig. 7C). Furthermore, we observed that TIP60 overexpression induced caspase 3 activation from its precursor pro-caspase 3 (Fig. 7A), which in turn triggered the cleavage of PARP to induce apoptosis.

In order to assess the effect of TIP60 overexpression on downstream signaling pathways of p73, we performed flow cytometry experiments. TIP60-eGFP transfected cells were analyzed by FACS and compared with cells treated with the transfection vector jetPEI. Propidium iodide (PI) and Annexin-V-iFluor™ 350 staining aided us to detect late and early phases of apoptosis. A significant decrease (34%) in cell viability was observed in TIP60- transfected cells as compared to control cells. Along with the decrease in cell viability after TIP60 overexpression, an increase of 12% and 16% in early and late apoptotic cells was also observed, respectively (Fig. 8A, B and C).

To confirm the above results, we separated the total population of TIP60-eGFP transfected cells into TIP60-eGFP positive and TIP60-eGFP negative cell populations based on the eGFP fluorescence. Average transfection efficiency of TIP60-eGFP was 61%, so that significant populations of both types of cells could be obtained. This separation allowed comparing apoptosis induction in TIP60-eGFP expressing cells and nonexpressing cells, in the same sample. Viability of TIP60-eGFP expressing cells was decreased by 39% as compared to cells not expressing TIP60-eGFP (Fig. 8D-F). In TIP60-eGFP transfected cells, there was also a strong increase in early and late apoptotic cells (Fig. 8E, F). As UHRF1 exhibits anti-apoptotic properties [5, 65], targeting UHRF1 expression can thus activate apoptotic pathways in cancer cells. Cumulatively, our data explain the correlation between TIP60-mediated down-regulation of the epigenetic integrator UHRF1 and induction of apoptosis in cancer cells to maintain the cellular and genomic integrity.

Discussion

UHRF1 and TIP60 are within the same epigenetic complex with other partners like DNMT1, USP7, HDAC1, PCNA (proliferating cell nuclear antigen) and G9a/EHMT2 (euchromatic histone-lysine N

methyltransferase 2) [17, 25, 27, 64, 69]. Higher expression levels of UHRF1 are reported in most cancer types [4, 70] and related to suppression of TSGs expression, tumor invasion, poor prognosis and resistance towards chemotherapy [4, 71, 72, 73, 74, 75]. In contrast to UHRF1, TIP60 expression is low in cancer cells. TIP60 is thought to have a tumor suppressor role by maintaining the cellular and genomic stability [25, 41, 45, 51, 52, 53, 54, 55, 56]. UHRF1 directly interacts with the MYST domain of TIP60 [57] and regulates TIP60 expression and activity [25, 27]. There is thus a fragile balance between UHRF1 and TIP60 broken in favour of UHRF1 in cancers. Thus, we believe that the role of TIP60 is to maintain UHRF1 at physiological levels in the UHRF1/DNMT1 macromolecular complex.

In the present study, we confirmed by Western blot and confocal microscopy that TIP60 down-regulates the UHRF1/DNMT1 tandem. Interestingly, the ΔMYST mutant (lacking acetyltransferase activity) was unable to impact the expression of both proteins, indicating that the acetyltransferase activity of TIP60 is required for down-regulating both proteins. We suggest that TIP60 drives the degradation of UHRF1 and consequently DNMT1, considering that this latter has been shown to be under the control of UHRF1 [76]. A direct control of TIP60 on DNMT1, in an USP7-dependent way, may also occur [17].

Ubiquitination is a post-translational modification which adds single or multiple ubiquitin molecules to proteins marking them for proteasomal degradation, cellular trafficking, autophagy, DNA repair, receptor internalization or regulation of enzymatic activity [77, 78]. USP7 is a deubiquitinating enzyme which protects many proteins from ubiquitination including p53, UHRF1, PTEN, MDM2 and Myc. Its expression levels are high in many cancers. Dysregulation in ubiquitylation/deubiquitylation can play a critical role in several diseases including cancer [77]. USP7 interacts with UHRF1 and protects it from degradation [58, 79] while during the M phase, UHRF1 is degraded as a result of its dissociation from USP7 [64]. Zhang *et al* reported that TIP60 acetylates UHRF1 at K659, which decreases the interaction of USP7-UHRF1 [58]. Our data showed that overexpression of TIP60 but not of its ΔMYST mutant interfered with the association and expression levels of USP7 and UHRF1. Dissociation of USP7 with UHRF1 likely condemns this latter becoming a prey for E3 ligases that have been reported to ubiquitinate UHRF1 [80, 81] or belong to the UHRF1 complex [15].

In the present study, we observed ubiquitination of UHRF1 after TIP60 overexpression which is likely a consequence of TIP60-mediated UHRF1-USP7 dissociation, as it has been reported for DNMT1 [17, 82]. Due to this dissociation, USP7 is no more able to protect UHRF1 from degradation through the proteasomal pathway. This hypothesis was confirmed by use of MG-132 that helped recovering initial UHRF1 levels. The RING domain of UHRF1 has E3 ligase activity through which it can either ubiquitinate itself or other proteins [16, 17]. Here we show that TIP60 overexpression controls auto-ubiquitination of UHRF1, but not of UHRF1 C724A-H741A mutant having impaired RING domain activity. Our data further indicated that the interaction between UHRF1 and ubiquitin occurred in a time dependent manner and that UHRF1 mutant, having impaired E3 ligase activity, was not able to interact with ubiquitin. We also found that TIP60 favor the UHRF1/ubiquitin interaction while inhibition of its acetyltransferase activity impairs this interaction. Subsequently, UHRF1 is degraded via the proteasome as a treatment with MG132 is able to recover initial UHRF1 levels.

A down-regulation of UHRF1 induces a recovering of numerous tumor suppressor genes including *RB1, p16INK4A (CDKN2A), CDH13, SOCS3, BRCA1, CDX2, RUNX3, FOXO4, PPGARG, PML* and *p73* [4, 24]. We focused on p73 as it is known that TIP60 positively regulates apoptosis [41] and that UHRF1 positively regulates p73 [66]. We found that TIP60 overexpression induced enhanced p73 expression. Therefore, we suggest that TIP60 mediated apoptosis is acting via an up-regulation of p73. However, we do not exclude that p73 is involved up-stream of TIP60 since it has been previously observed that p73 is also negatively regulating UHRF1 [83, 54]. Furthermore, in agreement with our study, it has been observed that p73 mediated apoptosis involves a caspase-dependent pathway [83].

Conclusions

In summary, we propose a model (Fig. 9) depicting the tumor suppressor role of TIP60. TIP60 up-regulation induced apoptosis by activation of p73 mediated downstream signaling pathway. TIP60 overexpression led to decrease BCL2 and increase BAX expression which activated Caspase-3. Caspase-3 activated the cleavage of PARP and induced apoptosis. Overall, our observations support a TSG role of TIP60 through the regulation of the auto-ubiquitination activity of UHRF1. This interplay directly governs the expression of TSGs, such as p73, explaining why TIP60 plays a role in apoptosis and cell cycle regulation.

Abbreviations

UHRF1
Ubiquitin-like, containing PHD and RING finger domains 1; TIP60:Tat interactive protein, 60 kDa; FLIM:Fluorescence lifetime imaging microscopy; DNMT1 (DNA methyltransferase 1), USP7:Ubiquitin-specific-processing protease 7; HDAC1:histone deacetylase 1; IP:Immunoprecipitation; WB:Western blotting; WT:Wild type; ΔMYST:MYST domain mutant; FRET:Förster Resonance Energy Transfer; PCNA:Proliferating cell nuclear antigen; EHMT2:Euchromatic histone-lysine N methyltransferase 2.

Declarations

Acknowledgments

We thank Romain Vauchelles (Plate-forme d'Imagerie Quantitative- PIQ) and Dr. Ludovic Richert for their help in Confocal and FLIM experiments, respectively.

Funding

This research was supported by ANR (SMFLUONA, ANR-17-CE11-0036-01). TA was supported by fellowships from Higher Education Commission (HEC), Pakistan. YM is grateful to the Institut Universitaire de France (IUF) for support and providing additional time to be dedicated to research.

Availability of data and materials

Please contact corresponding author for data requests.

Authors' contributions

TA conducted all the experiments with the help of WA, AI and LZ under the supervision of MM and CB. CDM helped in flow cytometry experiments. TA, CB, and MM wrote most of the manuscript with the guidance and help of AH and YM. All authors read and approved the final manuscript.

Ethics approval and consent to participate

Not applicable.

Consent for publication

Not applicable.

Competing interests

The authors declare that they have no competing interests.

References

1. Hopfner R, Mousli M, Jeltsch JM, Voulgaris A, Lutz Y, Marin C, Bellocq JP, Oudet P, Bronner C. ICBP90, a novel human CCAAT binding protein, involved in the regulation of topoisomerase IIalpha expression. Cancer Res. 2000;60(1):121–8.
2. Hopfner R, Mousli M, Garnier J-M, Redon R, du Manoir S, Chatton B, Ghyselinck N, Oudet P, Bronner C. Genomic structure and chromosomal mapping of the gene coding for ICBP90, a protein involved in the regulation of the topoisomerase IIα gene expression. Gene. 2001;266(1–2):15–23.
3. Krifa M, Alhosin M, Muller CD, Gies JP, Chekir-Ghedira L, Ghedira K, Mély Y, Bronner C, Mousli M. *Limoniastrum guyonianum* aqueous gall extract induces apoptosis in human cervical cancer cells involving p16 INK4A re-expression related to UHRF1 and DNMT1 down-regulation. J Exp Clin Cancer Res. 2013;32(1):30–40.
4. Ashraf W, Ibrahim A, Alhosin M, Zaayter L, Ouararhni K, Papin C, Ahmad T, Hamiche A, Mély Y, Bronner C, et al. The epigenetic integrator UHRF1: on the road to become a universal biomarker for cancer. Oncotarget. 2017;8(31):51946–62.

5. Bronner C, Achour M, Arima Y, Chataigneau T, Saya H, Schini-Kerth VB. The UHRF family: oncogenes that are drugable targets for cancer therapy in the near future? Pharmacol Ther. 2007;115(3):419–34.
6. Bostick M, Kim JK, Estève PO, Clark A, Pradhan S, Jacobsen SE. UHRF1 plays a role in maintaining DNA methylation in mammalian cells. Science. 2007;317(5845):1760–4.
7. Bronner C, Alhosin M, Hamiche A, Mousli M. Coordinated Dialogue between UHRF1 and DNMT1 to ensure faithful inheritance of methylated DNA patterns. Genes. 2019;10(1):65–78.
8. Avvakumov GV, Walker JR, Xue S, Li Y, Duan S, Bronner C, Arrowsmith CH, Dhe-Paganon S. Structural basis for recognition of hemi-methylated DNA by the SRA domain of human UHRF1. Nature. 2008;455(7214):822–5.
9. Sharif J, Muto M, Takebayashi S, Suetake I, Iwamatsu A, Endo TA, Shinga J, Mizutani-Koseki Y, Toyoda T, Okamura K, et al. The SRA protein Np95 mediates epigenetic inheritance by recruiting Dnmt1 to methylated DNA. Nature. 2007;450(7171):908–12.
10. Arita K, Ariyoshi M, Tochio H, Nakamura Y, Shirakawa M. Recognition of hemi-methylated DNA by the SRA protein UHRF1 by a base-flipping mechanism. Nature. 2008;455(7214):818–21.
11. Nady N, Lemak A, Walker JR, Avvakumov GV, Kareta MS, Achour M, Xue S, Duan S, Allali-Hassani A, Zuo X, et al. Recognition of multivalent histone states associated with heterochromatin by UHRF1 protein. J Biol Chem. 2011;286(27):24300–11.
12. Rajakumara E, Wang Z, Ma H, Hu L, Chen H, Lin Y, Guo R, Wu F, Li H, Lan F, et al. PHD finger recognition of unmodified histone H3R2 links UHRF1 to regulation of euchromatic gene expression. Mol Cell. 2011;43(2):275–84.
13. Hu L, Li Z, Wang P, Lin Y, Xu Y. Crystal structure of PHD domain of UHRF1 and insights into recognition of unmodified histone H3 arginine residue 2. Cell Res. 2011;21(9):1374–80.
14. Jenkins Y, Markovtsov V, Lang W, Sharma P, Pearsall D, Warner J, Franci C, Huang B, Huang J, Yam GC, et al. Critical Role of the Ubiquitin Ligase Activity of UHRF1, a Nuclear RING Finger Protein, in Tumor Cell Growth. Mol Biol Cell. 2005;16(12):5621–9.
15. Ibrahim A, Alhosin M, Papin C, Ouararhni K, Omran Z, Zamzami MA, Al-Malki AL, Choudhry H, Mély Y, Hamiche A, et al. Thymoquinone challenges UHRF1 to commit auto-ubiquitination: a key event for apoptosis induction in cancer cells. Oncotarget. 2018;9(47):28599–611.
16. Tauber M, Fischle W. Conserved linker regions and their regulation determine multiple chromatin-binding modes of UHRF1. Nucleus. 2015;6(2):123–32.
17. Du Z, Song J, Wang Y, Zhao Y, Guda K, Yang S, Kao HY, Xu Y, Willis J, Markowitz SD, et al. DNMT1 stability is regulated by proteins coordinating deubiquitination and acetylation-driven ubiquitination. Sci Signal. 2010;3(146):1–21.
18. Nishiyama A, Yamaguchi L, Sharif J, Johmura Y, Kawamura T, Nakanishi K, Shimamura S, Arita K, Kodama T, Ishikawa F, et al. Uhrf1-dependent H3K23 ubiquitylation couples maintenance DNA methylation and replication. Nature. 2013;502(7470):249–53.

19. Qin W, Wolf P, Liu N, Link S, Smets M, La Mastra F, Forné I, Pichler G, Hörl D, Fellinger K, et al. DNA methylation requires a DNMT1 ubiquitin interacting motif (UIM) and histone ubiquitination. Cell Res. 2015;25(8):911–29.
20. Foster BM, Stolz P, Mulholland CB, Montoya A, Kramer H, Bultmann S, Bartke T. Critical role of the UBL domain in stimulating the E3 ubiquitin ligase activity of UHRF1 toward chromatin. Mol Cell. 2018;72(4):739–52.
21. Mishima Y, Brueckner L, Takahashi S, Kawakami T, Otani J, Shinohara A, Takeshita K, Garvilles RG, Watanabe M, Sakai N, et al. Enhanced processivity of Dnmt1 by monoubiquitinated histone H3. Genes Cells. 2020;25(1):22–32.
22. Li T, Wang L, Du Y, Xie S, Yang X, Lian F, Zhou Z, Qian C. Structural and mechanistic insights into UHRF1-mediated DNMT1 activation in the maintenance DNA methylation. Nuclic Acids Res. 2018;46(6):3218–31.
23. Alhosin M, Omran Z, Zamzami MA, Al-Malki AL, Choudhry H, Mousli M, Bronner C. Signalling pathways in UHRF1-dependent regulation of tumor suppressor genes in cancer. J Exp Clin Cancer Res. 2016;35(1):174–84.
24. Alhosin M, Sharif T, Mousli M, Etienne-Selloum N, Fuhrmann G, Schini-Kerth VB, Bronner C. Down-regulation of UHRF1, associated with re-expression of tumor suppressor genes, is a common feature of natural compounds exhibiting anti-cancer properties. J Exp Clin Cancer Res. 2011;30(1):41–50.
25. Dai C, Shi D, Gu W. Negative regulation of the acetyltransferase TIP60-p53 interplay by UHRF1 (ubiquitin-like with PHD and RING finger domains 1). J Biol Chem. 2013;288(27):19581–95.
26. Guan D, Factor D, Liu Y, Wang Z, Kao HY. The epigenetic regulator UHRF1 promotes ubiquitination-mediated degradation of the tumor-suppressor protein promyelocytic leukemia protein. Oncogene. 2013;32(33):3819–28.
27. Achour M, Fuhrmann G, Alhosin M, Rondé P, Chataigneau T, Mousli M, Schini-Kerth VB, Bronner C. UHRF1 recruits the histone acetyltransferase Tip60 and controls its expression and activity. Biochem Biophys Res Commun. 2009;390(3):523–8.
28. Kamine J, Elangovan B, Subramanian T, Coleman D, Chinnadurai G. Identification of a Cellular Protein That Specifically Interacts with the Essential Cysteine Region of the HIV-1 Tat Transactivator. Virology. 1996;216(2):357–66.
29. Yamamoto T, Horikoshi M. Novel Substrate Specificity of the Histone Acetyltransferase Activity of HIV-1-Tat Interactive Protein Tip60. J Bioll Chem. 1997;272(49):30595–8.
30. Hilfiker A, Hilfiker-Kleiner D, Pannuti A, Lucchesi JC. Mof, a putative acetyl transferase gene related to the Tip60 and MOZ human genes and to the SAS genes of yeast, is required for dosage compensation in Drosophila. EMBO J. 1997;16(8):2054–60.
31. Lee KK, Workman JL. Histone acetyltransferase complexes: one size doesnot fit all. Nat Rev Mol Cell Biol. 2007;8:284–95.
32. Doyon Y, Selleck W, Lane WS, Tan S, Côté J. Structural and functional conservation of the NuA4 histone acetyltransferase complex from yeast to humans. Mol Cell Biol. 2004;24(5):1884–96.

33. Voss AK, Thomas T. MYST family histone acetyltransferases take center stage in stem cells and development. BioEssays 2009;31(10):1050–1061.
34. Sheikh BN, Akhtar A. The many lives of KATs — detectors, integrators and modulators of the cellular environment. Nat Rev Genet. 2019;20:7–23.
35. Kim CH, Kim JW, Jang SM, An JH, Seo S-B, Choi K-H. The chromodomain-containing histone acetyltransferase TIP60 acts as a code reader, recognizing the epigenetic codes for initiating transcription. Biosci Biotechnol Biochem. 2015;79(4):532–8.
36. Squatrito M, Gorrini C, Amati B. Tip60 in DNA damage response and growth control: many tricks in one HAT. Trends Cell Biol. 2006;16(9):433–42.
37. Kimura A, Matsubara K, Horikoshi M. A decade of histone acetylation: marking eukaryotic chromosomes with specific codes. J Biochem. 2005;138(6):647–62.
38. Kim MY, Ann EJ, Kim JY, Mo JS, Park JH, Kim SY, Seo MS, Park HS. Tip60 histone acetyltransferase acts as a negative regulator of Notch1 signaling by means of acetylation. Mol Cell Biol. 2007;27(18):6506–19.
39. Sapountzi V, Logan IR, Robson CN. Cellular functions of TIP60. Int J Biochem Cell Biol. 2006;38(9):1496–509.
40. Putnik J, Zhang CD, Archangelo LF, Tizazu B, Bartels S, Kickstein M, Greif PA, Bohlander SK. The interaction of ETV6 (TEL) and TIP60 requires a functional histone acetyltransferase domain in TIP60. Biochim Biophys Acta. 2007;1772(11–12):1211–24.
41. Ikura T, Ogryzko VV, Grigoriev M, Groisman R, Wang J, Horikoshi M, Scully R, Qin J, Nakatani Y. Involvement of the TIP60 histone acetylase complex in DNA repair and apoptosis. Cell. 2000;104(4):463–73.
42. Judes G, Rifaï K, Ngollo M, Daures M, Bignon YJ, Penault-Llorca F, Bernard-Gallon D. A bivalent role of TIP60 histone acetyl transferase in human cancer. Epigenomics. 2015;7(8):1351–63.
43. Mouhamed I, Khaldoun R, Marine D, Frédérique P-L, Yves-Jean B, Dominique B-G. Exciting History of Tip60 and Its Companions in Carcinogenesis Across the Heterochromatin Landscapes. OMICS: A J Integ Biol. 2018;22(9):626–628.
44. Frank SR, Parisi T, Taubert S, Fernandez P, Fuchs M, Chan HM, Livingston DM, Amati B. MYC recruits the TIP60 histone acetyltransferase complex to chromatin. EMBO Rep. 2003;4(6):575–80.
45. Berns K, Hijmans EM, Mullenders J, Brummelkamp TR, Velds A, Heimerikx M, Kerkhoven RM, Madiredjo M, Nijkamp W, Weigelt B, et al. A large-scale RNAi screen in human cells identifies new components of the p53 pathway. Nature. 2004;428(6981):431–7.
46. Mo F, Zhuang X, Liu X, Yao PY, Qin B, Su Z, Zang J, Wang Z, Zhang J, Dou Z, et al. Acetylation of Aurora B by TIP60 ensures accurate chromosomal segregation. Nat Chem Biol. 2016;12(4):226–32.
47. DeRan M, Pulvino M, Greene E, Su C, Zhao J. Transcriptional activation of histone genes requires NPAT-dependent recruitment of TRRAP-Tip60 complex to histone promoters during the G1/S phase transition. Mol Cell Biol. 2008;28(1):435–47.

48. Niida H, Katsuno Y, Sengoku M, Shimada M, Yukawa M, Ikura M, Ikura T, Kohno K, Shima H, Suzuki H, et al. Essential role of Tip60-dependent recruitment of ribonucleotide reductase at DNA damage sites in DNA repair during G1 phase. Genes Deve. 2010;24(4):333–8.
49. Taubert S, Gorrini C, Frank SR, Parisi T, Fuchs M, Chan HM, Livingston DM, Amati B. E2F-dependent histone acetylation and recruitment of the Tip60 acetyltransferase complex to chromatin in late G1. Mol Cell Biol. 2004;24(10):4546–56.
50. Hu Y, Fisher JB, Koprowski S, McAllister D, Kim MS, Lough J. Homozygous disruption of the Tip60 gene causes early embryonic lethality. Dev Dyn. 2009;238(11):2912–21.
51. Sakuraba K, Yasuda T, Sakata M, Kitamura YH, Shirahata A, Goto T, Mizukami H, Saito M, Ishibashi K, Kigawa G, et al. Down-regulation of Tip60 gene as a potential marker for the malignancy of colorectal cancer. Anticancer Res. 2009;29(10):3953–5.
52. Sakuraba K, Yokomizo K, Shirahata A, Goto T, Saito M, Ishibashi K, Kigawa G, Nemoto H, Hibi K. TIP60 as a potential marker for the malignancy of gastric cancer. Anticancer Res. 2011;31(1):77–9.
53. Gorrini C, Squatrito M, Luise C, Syed N, Perna D, Wark L, Martinato F, Sardella D, Verrecchia A, Bennett S, et al. Tip60 is a haplo-insufficient tumour suppressor required for an oncogene-induced DNA damage response. Nature. 2007;448(7157):1063–70.
54. Kim JH, Kim B, Cai L, Choi HJ, Ohgi KA, Tran C, Chen C, Chung CH, Huber O, Rose DW, et al. Transcriptional regulation of a metastasis suppressor gene by Tip60 and beta-catenin complexes. Nature. 2005;434(7035):921–6.
55. Jha S, Vande Pol S, Banerjee NS, Dutta AB, Chow LT, Dutta A. Destabilization of TIP60 by human papillomavirus E6 results in attenuation of TIP60-dependent transcriptional regulation and apoptotic pathway. Mol Cell. 2010;38(5):700–11.
56. Brown JA, Bourke E, Eriksson LA, Kerin MJ. Targeting cancer using KAT inhibitors to mimic lethal knockouts. Biochem Soc Trans. 2016;44(4):979–86.
57. Ashraf W, Bronner C, Zaayter L, Ahmad T, Richert L, Alhosin M, Ibrahim A, Hamiche A, Mely Y, Mousli M. Interaction of the epigenetic integrator UHRF1 with the MYST domain of TIP60 inside the cell. J Exp Clin Cancer Res. 2017;36:188–201.
58. Zhang ZM, Rothbart SB, Allison DF, Cai Q, Harrison JS, Li L, Wang Y, Strahl BD, Wang G, et al. An allosteric interaction links USP7 to deubiquitination and chromatin targeting of UHRF1. Cell Re. 2015;12(9):1400–6.
59. Cheng J, Yang H, Fang J, Ma L, Gong R, Wang P, Li Z, Xu Y. Molecular mechanism for USP7-mediated DNMT1 stabilization by acetylation. Nat Commun. 2015;6:7023–33.
60. Clamme JP, Azoulay J, Mély Y. Monitoring of the formation and dissociation of polyethylenimine/DNA complexes by two photon fluorescence correlation spectroscopy. Biophys J. 2003;84(3):1960–8.
61. El Meshri SE, Dujardin D, Godet J, Richert L, Boudier C, Darlix JL, Didier P, Mély Y, de Rocquigny H. Role of the nucleocapsid domain in HIV-1 Gag oligomerization and trafficking to the plasma

membrane: a fluorescence lifetime imaging microscopy investigation. J Mol Biol. 2015;427(6):1480–94.

62. Becker W. Advanced time-correlated single photon counting applications. Heidelberg: Springer; 2015.
63. Voss TC, Demarco IA, Day RN. Biotechniques. 2005;38:413–24.
64. Ma H, Chen H, Guo X, Wang Z, Sowa ME, Zheng L, Hu S, Zeng P, Guo R, Diao J, et al. M phase phosphorylation of the epigenetic regulator UHRF1 regulates its physical association with the deubiquitylase USP7 and stability. Proc Natl Acad Sci. 2012;109(13):4828–33.
65. Alhosin M, Abusnina A, Achour M, Sharif T, Muller C, Peluso J, Chataigneau T, Lugnier C, Schini-Kerth VB, Bronner C, et al. Induction of apoptosis by thymoquinone in lymphoblastic leukemia Jurkat cells is mediated by a p73-dependent pathway which targets the epigenetic integrator UHRF1. Biochem Pharmacol. 2010;79(9):1251–60.
66. Achour M, Mousli M, Alhosin M, Ibrahim A, Peluso J, Muller CD, Schini-Kerth VB, Hamiche A, Dhe-Peganon S, Bronner C. Epigallocatechin-3-gallate Up-Regulates Tumor Suppressor Gene Expression via a Reactive Oxygen Species-Dependent Down-Regulation of UHRF1. Biochem Biophys Res Commun. 2013;4(1):208–12.
67. Léon-Gonzàlez J, José A, Jara-Palacios M, Abbas M, Heredia J, Schini-Kerth F. VB. Role of epigenetic regulation on the induction of apoptosis in Jurkat leukemia cells by white grape pomace rich in phenolic compounds. Food Nut. 2017;8(11):4062–9.
68. Sharif T, Alhosin M, Auger C, Minker C, Kim JH, Etienne-Selloum N, Bories P, Gronemeyer H, Lobstein A, Bronner C, et al. *Aronia melanocarpa* Juice Induces a Redox-Sensitive p73-Related Caspase 3-Dependent Apoptosis in Human Leukemia Cells. PLoS One. 2012;7(3):1–11.
69. Kim JK, Estève P-O, Jacobsen SE, Pradhan S. UHRF1 binds G9a and participates in p21 transcriptional regulation in mammalian cells. Nucleic Acids Res. 2009;37(2):493–505.
70. Polepalli S, George SM, Valli Sri Vidya R, Rodrigues GS, Ramachandra L, Chandrashekar R, MD N, Rao PPN, Pestell RG, Rao M. Role of UHRF1 in malignancy and its function as a therapeutic target for molecular docking towards the SRA domain. Int J Biochem Cell Biol. 2019;114:105558.
71. Boukhari A, Alhosin M, Bronner C, Sagini K, Truchot C, Sick E, Schini-Kerth VB, André P, Mély Y, Mousli M, et al. CD47 activation-induced UHRF1 over-expression is associated with silencing of tumor suppressor gene p16INK4A in glioblastoma cells. Anticancer Res. 2015;35(1):149–57.
72. Jeanblanc M, Mousli M, Hopfner R, Bathami K, Martinet N, Abbady AQ, Siffert JC, Mathieu E, Muller CD, Bronner C. The retinoblastoma gene and its product are targeted by ICBP90: a key mechanism in the G1/S transition during the cell cycle. Oncogene. 2005;24:7337–45.
73. Unoki M, Brunet J, Mousli M. Drug discovery targeting epigenetic codes: the great potential of UHRF1, which links DNA methylation and histone modifications, as a drug target in cancers and toxoplasmosis. Biochem Pharmacol. 2009;78(10):1279–88.
74. Wang F, Yang YZ, Shi CZ, Zhang P, Moyer MP, Zhang HZ, Zou Y, Qin HL. UHRF1 promotes cell growth and metastasis through repression of p16(inkâ´a) in colorectal cancer. Ann Surg Oncol. 2012;19(8):2753–62.

75. Xue B, Zhao J, Feng P, Xing J, Wu H, Li Y. Epigenetic mechanism and target therapy of UHRF1 protein complex in malignancies. OncoTargets Ther. 2019;12:549–59.
76. Achour M, Jacq X, Rondé P, Alhosin M, Charlot C, Chataigneau T, Jeanblanc M, Macaluso M, Giordano A, Hughes AD, et al. The Interaction of the SRA Domain of ICBP90 With a Novel Domain of DNMT1 Is Involved in the Regulation of VEGF Gene Expression. Oncogene. 2008;27(15):2187–97.
77. Gao Y, Wang Y, Zhou C, Kong S, Lu J, Wang H, Yang J. Ubiquitin-specific protease 7 (USP7) is essential for endometrial stromal cell decidualization in mice. Deve Growth Diff. 2019;61:176–85.
78. Popovic D, Vucic D, Dikic I. Ubiquitination in disease pathogenesis and treatment. Nature Med. 2014;20(11):1242–53.
79. Felle M, Joppien S, Németh A, Diermeier S, Thalhammer V, Dobner T, Kremmer E, Kappler R, Längst G. The USP7/Dnmt1 complex stimulates the DNA methylation activity of Dnmt1 and regulates the stability of UHRF1. Nucleic Acids Res. 2011;39(19):8355–65.
80. Mistry H, Gibson L, Yun JW, Sarras H, Tamblyn L, McPherson JP. Interplay Between Np95 and Eme1 in the DNA Damage Response. Biochem Biophys Res Commun. 2008;375(3):321–5.
81. Chen H, Ma H, Inuzuka H, Diao J, Lan F, Geno Shi Y, Wei W, Shi Y. DNA Damage Regulates UHRF1 Stability via the SCF(β-TrCP) E3 Ligase. Mol Cell Biol. 2013;33(6):1139–48.
82. Bronner C. Control of DNMT1 Abundance in Epigenetic Inheritance by Acetylation, Ubiquitylation, and the Histone Code. Sci Sign. 2013;4(157):1–3.
83. Jang SY, Hong D, Jeong SY, Kim Jong-H. Shikonin Causes Apoptosis by Up-Regulating p73 and Down-Regulating ICBP90 in Human Cancer Cells. Biochem Biophys Res Commun. 2015;465(1):71–6.

Figures

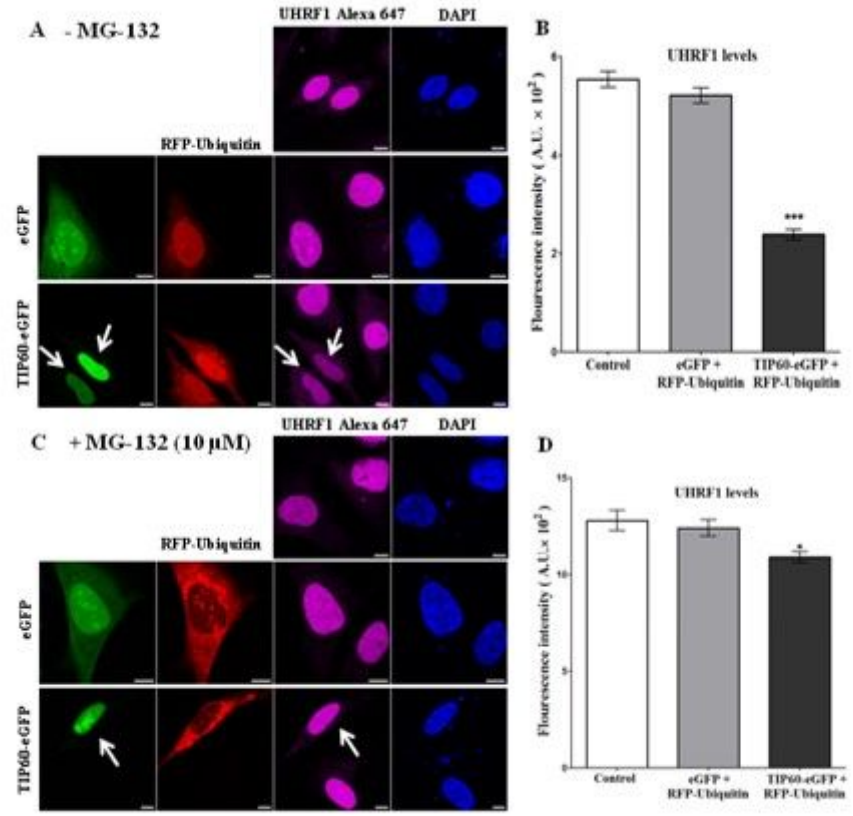

Figure 1

TIP60 and ubiquitin co-transfection induces down-regulation of UHRF1. Cells were co-transfected with either TIP60-eGFP (green) and RFP-Ubiquitin (red) or eGFP and RFP-Ubiquitin. Immunostaining of UHRF1 in HeLa cells without (A) or with treatment by MG-132 (C). Cells were fixed after transfection and labeled with anti-UHRF1 antibody. Endogenous UHRF1 protein was labeled with Alexa 647-labeled secondary antibody before visualization in confocal microscopy. White arrows indicate the TIP60-eGFP transfected cells and white bar indicates size of 10 µm. B and D represent mean fluorescence intensities levels of UHRF1 in the different samples. Values are means ± S. E. M. for three independent experiments; statistically significant: * $p < 0.05$; *** $p < 0.001$ (versus control group).

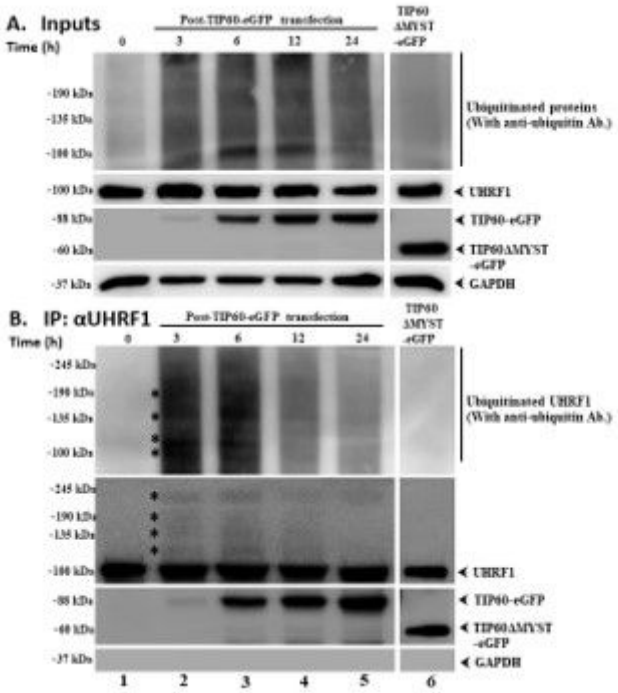

Figure 2

TIP60 induces UHRF1 ubiquitination in HeLa cells. Cells were co-transfected with either TIP60-eGFP WT or TIP60ΔMYST-eGFP mutant. All samples were treated with 10 μM of MG-132 for 8 h before harvesting the cells (In case of 3 and 6 h sample, MG-132 was added 5 and 2 h before transfection, respectively). Cells were collected 3, 6, 12 and 24 h post TIP60 transfection and 24 h in case of TIP60ΔMYST mutant. IP was performed with anti-UHRF1 antibody. Inputs and IP samples were analyzed by SDS-PAGE and then immunoblotted with anti-UHRF1 and anti-Ubiquitin antibodies. Stars indicate ubiquitinated UHRF1 bands.

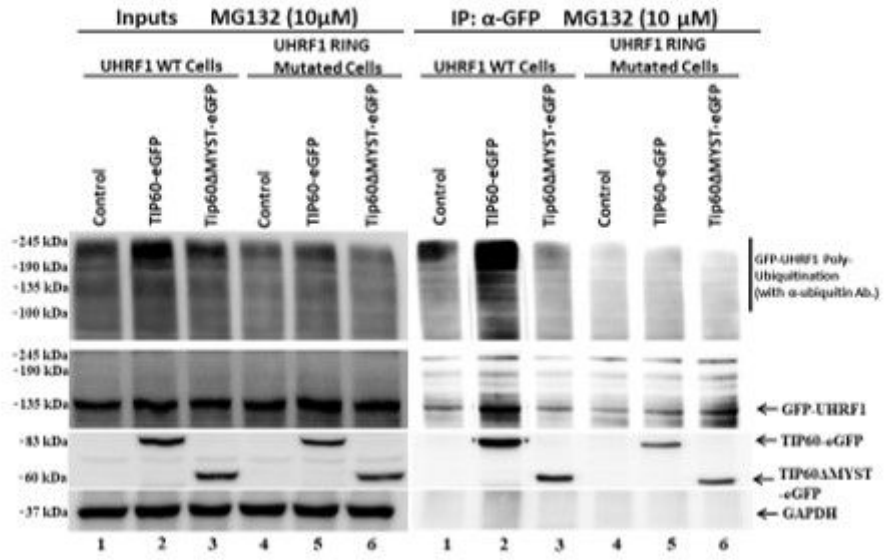

Figure 3

TIP60 induces auto-ubiquitination of UHRF1 in HeLa cells. Cells stably expressing either UHRF1 WT or UHRF1 C724A-H741A mutant were transfected with either TIP60-His WT or TIP60ΔMYST-His mutant. All samples were treated with 10 μM of MG-132, 8 h before harvesting the cells. Whole cell lysates and immunoprecipitated samples were analyzed by SDS-PAGE and then immunoblotted with anti-GFP and anti-Ubiquitin antibodies.

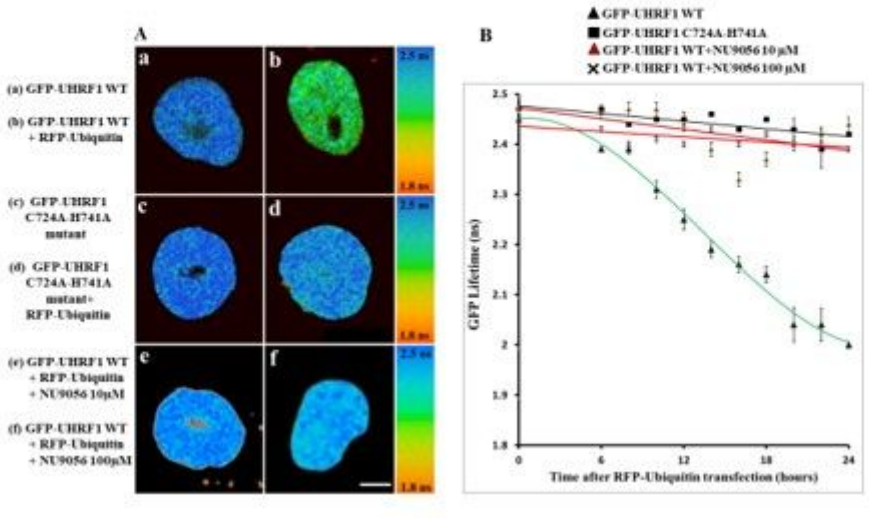

Figure 4

Interaction of UHRF1 and Ubiquitin, as determined by FRET-FLIM. (A) Representative 30 μm x 30 μm FLIM images of HeLa cells stably expressing GFP-UHRF1 WT (a) and co-transfected with RFP-ubiquitin (b), HeLa cells stably expressing GFP-UHRF1 C724A-H741A (c) and co-transfected with RFP-ubiquitin (d). The lifetime values are shown by a color code ranging from red (1.8 ns) to blue (2.5 ns). White bar indicates size of 10 μm. In comparison to cells expressing only GFP-UHRF1 WT (a), a strong decrease in GFP lifetime and thus, a strong FRET efficiency was observed when HeLa cells were transfected with RFP-ubiquitin (b). In contrast, no significant difference in lifetime or FRET efficiency was observed when HeLa cells expressing GFP-UHRF1 C724A-H741A were transfected with RFP-ubiquitin (compare d with c). No significant difference in lifetime or FRET efficiency was observed in HeLa cells expressing GFP-UHRF1 WT in the presence of the TIP60 inhibitor NU9056 10 μM (e) or 100 μM (f). FLIM data indicate that UHRF1 interacts with ubiquitin while this interaction is impaired in case of UHRF1 having a RING Finger domain mutation. (B) Change in GFP lifetime as a function of time. Values are means ± S.E.M. from 2 independent experiments. The fluorescence lifetimes of GFP-UHRF1 WT (without and with TIP60 inhibitor NU9056 10 μM, 100 μM) or GFP-UHRF1 C724A-H741A were measured at different times after transfection with RFP-Ubiquitin.

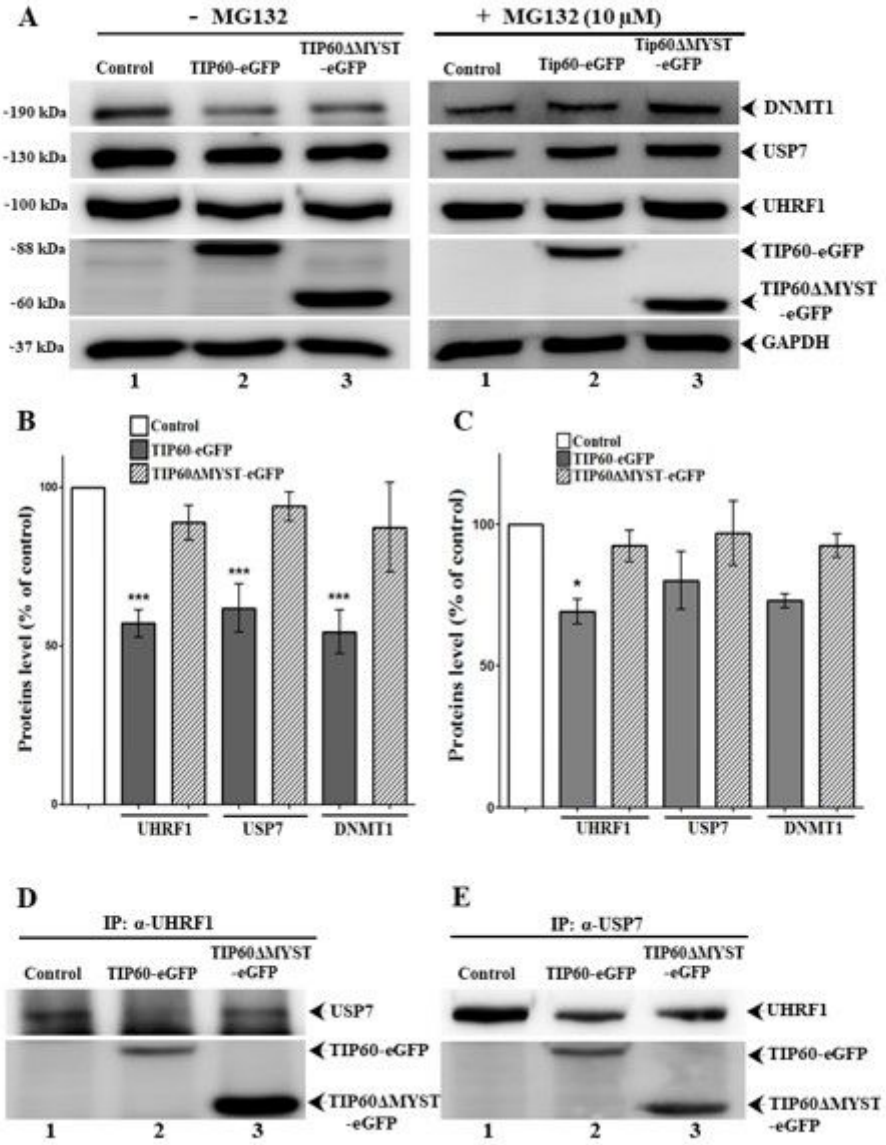

Figure 5

TIP60 interferes with UHRF1-USP7 association and their expression levels. HeLa cells were transfected with either TIP60-eGFP WT or TIP60ΔMYST-eGFP mutant. Western blot and immunoprecipitated samples were resolved by SDS-PAGE and immunoblotted with anti-UHRF1, anti-USP7 and anti-DNMT1 antibodies. (B and C) show the effect of TIP60 on UHRF1, USP7 and DNMT1 levels with or without MG-132 treatment, respectively. Results indicated are from five independent experiments which are analyzed statistically by one-way ANOVA (* $p < 0.05$; ** $p < 0.01$; *** $p < 0.001$ versus control group). (D) Anti-UHRF1 antibody was used to co-immunoprecipitate UHRF1 and its partner USP7. (E) In reciprocal experiment, anti-USP7 antibody was used to co-immunoprecipitate USP7 and UHRF1.

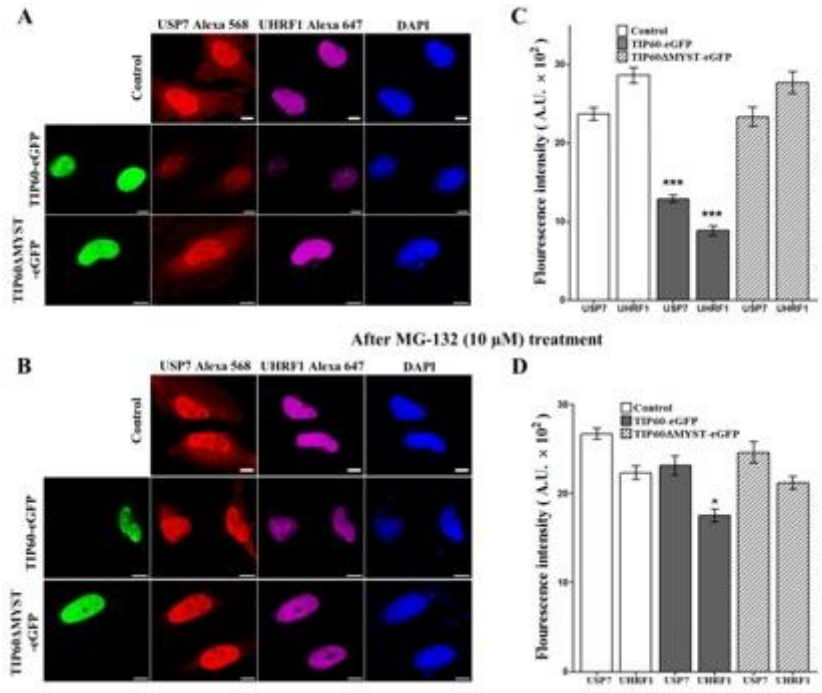

Figure 6

TIP60 down-regulates UHRF1 and USP7 levels in HeLa cells. Cells were either not treated with MG-132 or (A) or treated with MG-132 10 μM for 8 hours (B). Cells were immunostained with anti-USP7 or anti-UHRF1 antibodies. TIP60-eGFP wild type (WT) or TIP60ΔMYST-eGFP mutant was transiently overexpressed and their effects were compared with non-transfected control cells. Cells were fixed after transfection and tagged by anti-USP7 and anti-UHRF1 antibodies. Alexa 568 and Alexa 647-labeled secondary antibodies were used as indicated in the figure to visualize the corresponding proteins by confocal microscopy. White bar indicates size of 10 μm. (C and D) show the mean fluorescence intensities representing the levels of USP7 and UHRF1 before and after MG-132 treatment, respectively. Values are means ± S. E. M. for three independent experiments; statistically significant: * $p < 0.05$; ** $p < 0.01$; *** $p < 0.001$ (versus control group).

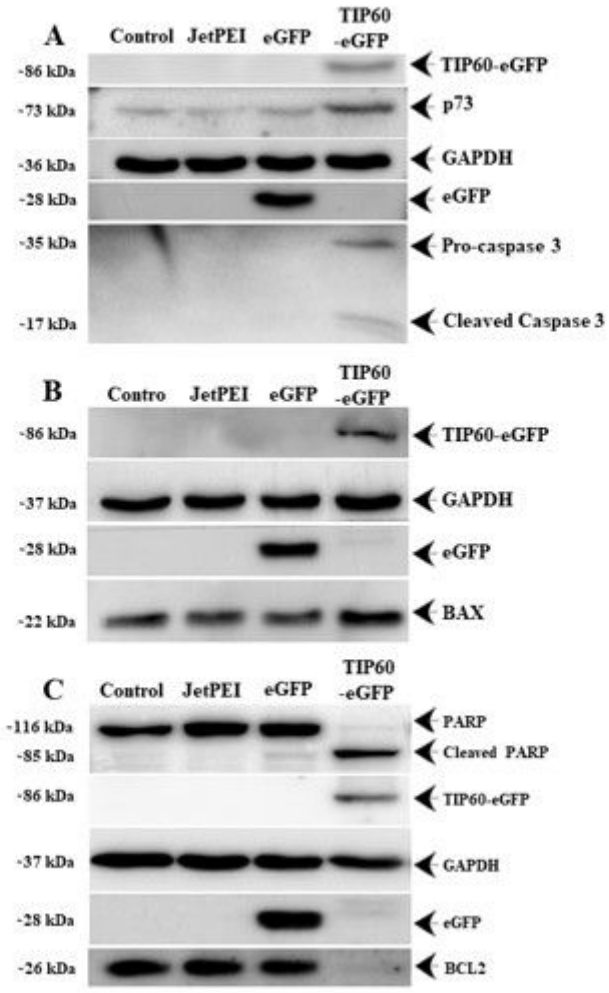

Figure 7

Effect of TIP60 overexpression on p73, and pro- and anti-apoptotic proteins. (A) p73 and Caspase 3 (B) BAX, (C) BCL2 and PARP levels were analyzed by Western blot after TIP60 overexpression in HeLa cells.

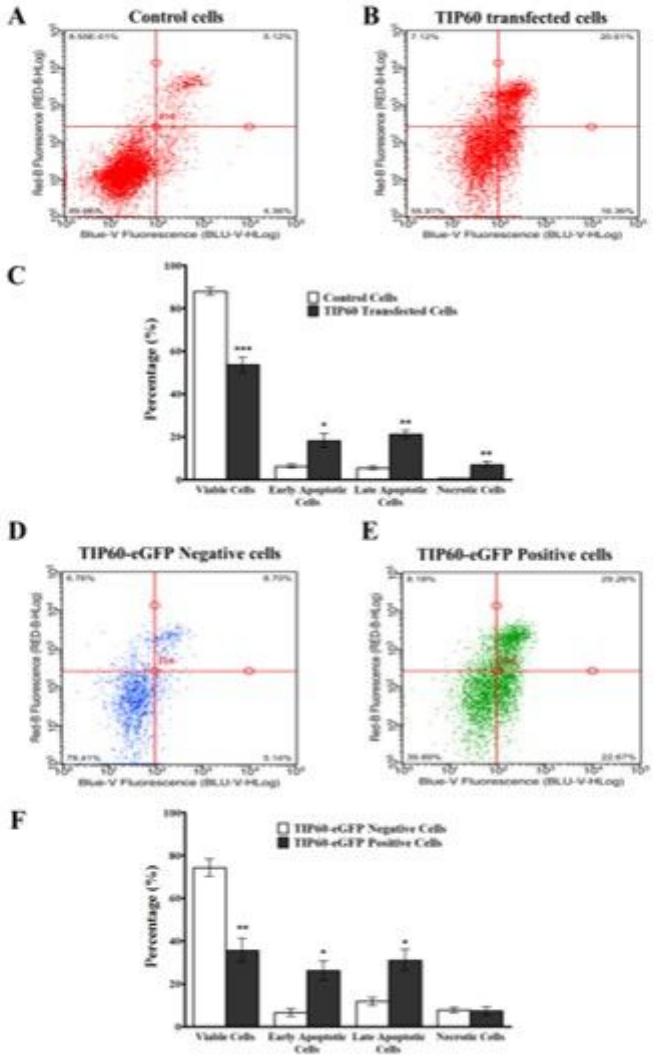

Figure 8

TIP60 overexpression induces apoptosis in cancer cells. (A) FACS analysis examining Annexin V-iFluor™ 350 and PI labeling in control HeLa cells (treated with jetPEI in identical manner) and (B) cells transfected with TIP60-eGFP for 24 hr. (D and E) FACS analysis examining Annexin V-iFluor™ 350 and PI labeling in TIP60-eGFP negative cells to TIP60-eGFP positive cells in TIP60-eGFP transfected samples. (C and F) Graph represents average values from three independent experiments which were statistically analyzed by Student's t-test (* $P < 0.05$; ** $P < 0.01$; *** $P < 0.001$).

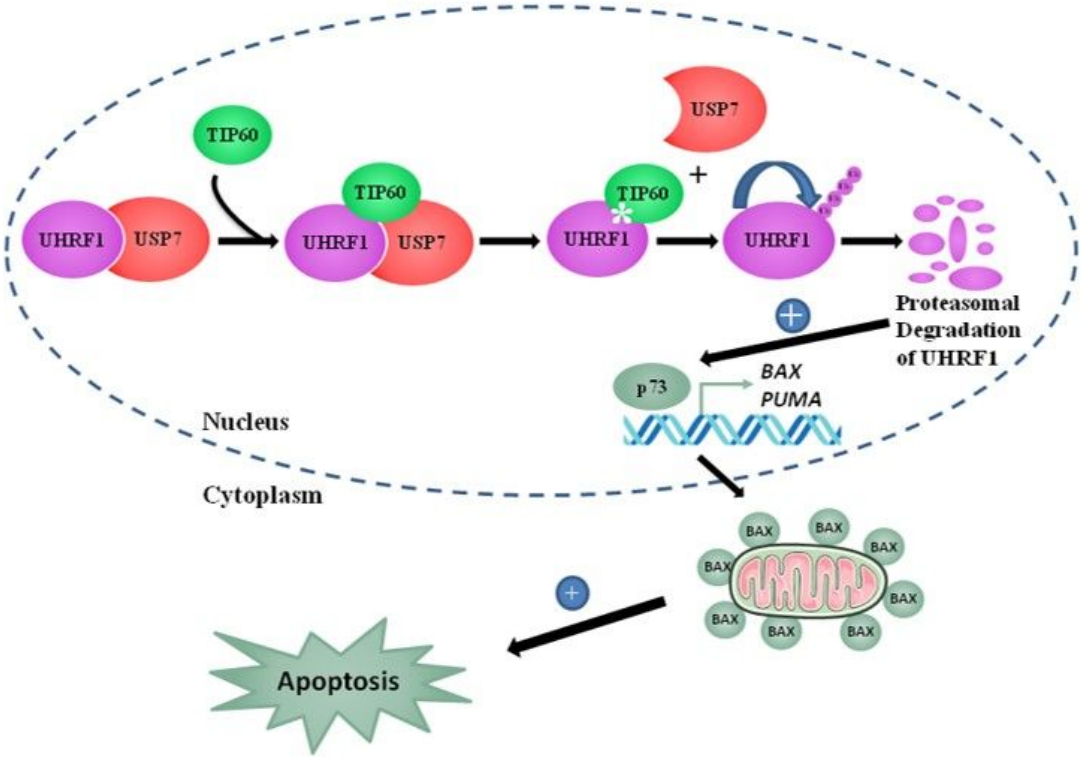

Figure 9

Schematic model of TIP60-mediated apoptosis in cancer cells. Association of UHRF1 with USP7 protects UHRF1 protein from proteasomal degradation. TIP60 overexpression disrupts the tandem UHRF1-USP7 which leads UHRF1 to commit suicide via auto-ubiquitination.

Supplementary Files

This is a list of supplementary files associated with this preprint. Click to download.

- SupportingInformationJECCR06082020.docx